



Numerical Simulation of Two Dimensional Unsteady Flow By Total Variation Diminishing Scheme

Amin GHAREHBAGHI ^{1,*}, Birol KAYA ² and Hamid SAADATNEJADGHARAHASSANLOU ³

^{1,2} Dokuz Eylül University, Department of Civil Engineering, Faculty of Engineering, Izmir, Turkey.

³ Islamic Azad University, Department of Civil Engineering, AHAR Branch, Tabriz, East Azerbaijan, Iran.

*e-mail: gharehbaghi.amin@gmail.com

Received date: June 2016

Accepted date: August 2016

Abstract

In recent years, many researchers have suggested various numerical techniques to solve the engineering problems like fluid flow intricacies. The objective of this paper is to introduce a numerical approach to simulate treatment of incompressible fluid flow in two-dimensional unsteady flow with the shallow water equations system. The governing equations were solved by Finite Volume Method in explicit conditions. Moreover, to discretize the governing equations, total variation diminishing scheme was employed in the unstructured triangular grid systems, directly. For evaluating the numerical results of developed model, the Flow3D software was used. In this direction, two hypothetical cases have been developed to investigate the accuracy of the results of the suggested model by Flow3D software. The comparison between numerical results of developed model and simulations of Flow3D software, shows good agreement. Furthermore, the suggested model can obtain acceptable results with less number of meshes than Flow3D software.

Keywords: Finite Volume Method, Two-Dimensional, Shallow Water Equations.

1. Introduction

In recent years with the development of computer science, researchers show more interest to use novel numerical techniques in Computational Fluid Dynamics (CFD) domain that led to the significant advances. Treatment of fluid flow in open channels and rivers can be predicted by two sets of hyperbolic systems of equations, which are called the Navier–Stokes Equations (NSE) system and Shallow Water Equations (SWE) system. Because of the complexity of the NSE's system, most researchers prefer to employ the SWE's system. Actually, the SWE's system is a simplified form of NSE's system. Many researchers like [1-5], tried to solve One-Dimensional (1D) SWE's system to determine the water surface profiles in open channels and rivers. However, the 1D models were not able to satisfy the complicated problems. Therefore, researchers preferred to develop novel models in the 2D or 3D domain. Researchers have employed different numerical techniques to solve the SWE's system, which the Finite Difference Method (FDM), Finite Element Method (FEM) and Finite Volume Method (FVM) are among the most common methods used in this field. In order to obtain reliable results for flow treatment, especially in irregular and curvilinear geometry, developing unstructured mesh is almost necessary. Since applying an unstructured mesh to FDM is quite difficult, so most methods were suggested by FEM or FVM. Additionally, the result of FDM, in the same order, number of mesh nodes and time steps, is less sensitive than other ones [6]. Although, applying mesh to the complex geometry by FEM is applicable, but implementation the FEM is not as uncomplicated as the FVM. Moreover, FVM is able to keep the balance of the amount of mass and momentum by solving the integral form of the conservation equations. In addition, FVM does not require a continuous form of computational domain. Thus, with regards to the points mentioned above, in this study FVM was selected as discretization method. A brief review of studies in this area is given as below:

Bradford et al. [7] introduced a model that could solve the 2D shallow-water flow over arbitrary topography with FVM. In this model, for determination the governing equations, Roe's approximate Riemann solver was used. Furthermore, the monotone upstream scheme for conservation laws and predictor-corrector for time steps were employed. Finally, the suggested model was tested by analytical solutions and experimental data. They announced that the result of the examination was in good agreement with analytical and experimental studies. Pan et al. [8] solved the 2D SWE's system by FVM in unstructured mesh. They used exact Riemann solver to calculate numerical flux from the interface between cells, and the improved form of dry Riemann solver was employed to deal with the wet/dry problems. They reported that the comparison among the results of improved model, and some typical examples and the tidal bore on the Qiantang River was acceptable. Chen et al. [9] presented a model that could solve the 2D two-layer SWE's system in explicit conditions. For estimating the Godunov flux and solving the Riemann problem approximately, that introduced by Harten, Lax and van Leer, they used HLL scheme. Additionally, they used bottom slope by lateralizing the momentum flux. Finally, they employed the Strang splitting to manage the frictional source term. Kesserwani et al. [10] proposed a novel high-resolution finite element scheme to solve 2D depth-integrated SWE's system. In this work, they employed the HLLC scheme of Riemann solver to calculate the upwind inter-cell fluxes. The implicit discretization for the finite element approximating coefficients was implemented to calculate the Friction forces. Touma et al. [11] introduced a novel 1D and 2D un-staggered central FVM for solving the SWE's system on flat and variable bottom topographies. In this research, the second-order accuracy in space and time has been achieved. Finally, they announced that the suggested

model showed good agreement with SWE problems. Canestrelli et al. [12] a non-conservative well-balanced FORCE-type scheme to solve multidimensional non-conservative equations such as the SWE's system. As a benefit of this method, they reported that non-conservative well-balanced FORCE-type schemes were able to solve the equations without requiring to the very refined mesh when the channel was strongly meandering. Ata et al. [13] used Weighted Average Flux (WAF) scheme on the SWE's system to solve problems with real bathymetry on the unstructured meshes. In this work, they used vertex-centered FVM by Harten-Lax-van Leer-Contact (HLLC) Riemann solver. Eventually, they compared the results by HLLC, Roe and Kinetic type schemes.

In the present study, to fill the gap of experimental data and test the results of proposed model, Flow3D software was employed to simulate 2D water surface profiles. Many of researchers like [14-17 , among many] employed this software in experimental and numerical investigations. In this paper, Total Variation Diminishing (TVD) scheme was employed in the SWE's system. According to the literature, the basic upwind differencing scheme introduces a high level of false diffusion due to its low order of accuracy (first-order) [18]. "Higher-order schemes such as central differencing and QUICK can give spurious oscillations or 'wiggles' when the Peclet number is high. When such higher-order schemes are used to solve turbulent quantities, e.g. turbulence energy and rate of dissipation, wiggles can give physically unrealistic negative values and instability. TVD schemes are designed to address this undesirable oscillatory behavior of higher-order schemes. In TVD schemes the tendency towards oscillation is counteracted by adding an artificial diffusion fragment or by adding a weighting towards upstream contribution" [18].

In this research, a coupled model with three components was used to predict the water surface profiles in open channels and rivers. The first component, named meshing component, was employed to develop unstructured triangular meshes for discretization the domain of the channel. The second component, called hydrodynamic component, was applied to calculate hydraulic data in the SWE's system. The third and final component, named results component, writes the results and draw the figures. The novelty of this research is directly employing of TVD scheme to discretize the governing equations without any solver. In addition, the suggested model can solve the governing equations by less number of meshes than Flow3D software.

2. Governing Equations

The general form of the 2D SWE's system for the prediction of water surface profiles is given as below,

$$\frac{\partial Q}{\partial t} + \frac{\partial F_1}{\partial x_1} + \frac{\partial F_2}{\partial x_2} = S \quad (1)$$

$$Q = \begin{bmatrix} h \\ q_1 \\ q_2 \end{bmatrix} \quad (2)$$

$$F_1 = \begin{bmatrix} q_1 \\ \frac{q_1^2}{h} + \frac{1}{2}gh^2 \\ \frac{q_1q_2}{h} \end{bmatrix} \quad (3)$$

$$F_2 = \begin{bmatrix} q_2 \\ \frac{q_1q_2}{h} \\ \frac{q_2^2}{h} + \frac{1}{2}gh^2 \end{bmatrix} \quad (4)$$

$$S = \begin{bmatrix} 0 \\ gh(s_{0,1} - S_{f,1}) \\ gh(s_{0,2} - S_{f,2}) \end{bmatrix} \quad (5)$$

Which, Q is the conserved vector (the time derivative of the components), F_1 and F_2 are the vectors of flux variables (derivation of the components) in the flow (x) and transect (y) directions, respectively, and S is the source term. g is the gravity acceleration. h is the depth of water. $S_{0,1}$, $S_{0,2}$ are the bed slopes in the flow (x) and transect (y) directions, respectively, and q_1 and q_2 are discharge per unit width in the flow (x) and transect (y) directions, respectively, Which,

$$\begin{cases} q_1 = u_1 \cdot h \\ q_2 = u_2 \cdot h \end{cases} \quad (6a, b)$$

Which, u_1 and u_2 are the components of the depth averaged velocity in the flow (x) and transect (y) directions, respectively. Furthermore, $S_{f,1}$, $S_{f,2}$ are friction slopes in the flow (x) and transect (y) directions, respectively, and is presented as follows

$$\begin{cases} S_{f,1} = \frac{n_m^2 u_1 \sqrt{u_1^2 + u_2^2}}{h^{4/3}} \\ S_{f,2} = \frac{n_m^2 u_2 \sqrt{u_1^2 + u_2^2}}{h^{4/3}} \end{cases} \quad (7a, b)$$

Which, n_m is the Manning's roughness coefficient.

3. Discretization Techniques With FVM

A triangular cell-centered FVM, was developed to discretize the governing equations. This discretization method applied in an unstructured mesh system. By using the divergence theorem, the Eq. (1) can be rewritten as follows,

$$\iint_{\Omega} \frac{dQ}{dt} + \int_{\partial\Omega} F \cdot n dl = \iint_{\Omega} S dW \quad (8)$$

Where, n is the unit outward vector normal to the boundary elements $\partial\Omega$, dl and dW are the arc elements and area elements, respectively. F is the vector of normal flux, which is equal to $F = [F_1, F_2]^T$. By assuming the constant and averaged value of Q in the center of each cell, the result of discretization can be yielded to the basic form as,

$$A \frac{dQ}{dt} + \sum_{m=1}^M F_n^m \cdot L^m = AS \quad (9)$$

Where, A is the area of each triangular shaped cells, m is the number of side of each cells, F_n^m is the normal of flux to each side of cells, and L^m is the length of the m -th component of each cells. The illustration of FV triangular domain is given in the Figure (1).

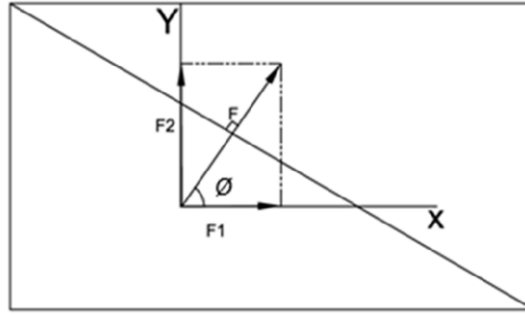


Fig. 1 Illustration of FV triangular domain

By assuming the counterclockwise angle of the x axis and n direction, which can be called as (ϕ) , and by employing the rotational invariance to the governing equations the normal of intercell flux of each side of the cell is given as,

$$F_n(Q) = F_1 \cos \phi + F_2 \sin \phi = T(\phi)^{-1} F [T(\phi) Q] = T(\phi)^{-1} F(\bar{Q}) \quad (10)$$

$$\bar{Q} = \begin{bmatrix} h \\ hu_n \\ hv_n \end{bmatrix} \quad (11)$$

$$F(\bar{Q}) = \begin{bmatrix} hu_n \\ \frac{\rho h^2}{2} + hu_n^2 \\ hu_n v_n \end{bmatrix} \quad (12)$$

$$T(\phi) = \begin{bmatrix} 1 & 0 & 0 \\ 0 & \cos \phi & \sin \phi \\ 0 & -\sin \phi & \cos \phi \end{bmatrix} \quad (13)$$

$$T(\phi)^{-1} = \begin{bmatrix} 1 & 0 & 0 \\ 0 & \cos \phi & -\sin \phi \\ 0 & \sin \phi & \cos \phi \end{bmatrix} \quad (14)$$

$$\begin{cases} u_n = u \cos \phi + v \sin \phi \\ v_n = v \cos \phi - u \sin \phi \end{cases} \quad (15a, b)$$

$\bar{Q} = T(\phi) Q$ is the transformed form of Q , $F(\bar{Q})$ is the transformed form of normal flux, $T(\phi)$ and $T(\phi)^{-1}$ are the matrices of transformation and inverse transformation, respectively. By some manipulation and substitution, the Equation (9) can be expressed as follows,

$$A \frac{dQ}{dt} + \sum_{m=1}^M T(\phi)^{-1} F(\bar{Q}) L^m = AS \quad (16)$$

It is important to mention that in the Equation (16), the key point is proposing a method to determine the value of $F(\bar{Q})$.

4. TVD Scheme

The illustration of 1D standard control volume is given in Figure (2).

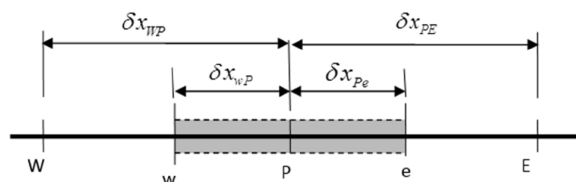


Fig. 2 Illustration of 1D standard control volume [18]

The east face value of upwind differencing (UD) scheme is given as follows

$$\mathbb{V}_e = \mathbb{V}_P \quad (17)$$

The east faces value of linear upwind differencing (LUD) scheme, is given as

$$\mathbb{V}_e = \mathbb{V}_P + \frac{\delta x (\mathbb{V}_P - \mathbb{V}_W)}{2 \delta x} = \mathbb{V}_P + \frac{1}{2} (\mathbb{V}_P - \mathbb{V}_W) \quad (18)$$

For the Quadratic Upstream Interpolation for Convective Kinematics (QUICK) scheme, the east face value can be yielded as follows

$$\mathbb{V}_e = \frac{6}{8} \mathbb{V}_P + \frac{3}{8} \mathbb{V}_E - \frac{1}{8} \mathbb{V}_W = \mathbb{V}_P + \frac{1}{8} (3\mathbb{V}_E - 2\mathbb{V}_P - \mathbb{V}_W) \quad (19)$$

This can be thought of as a second-order extension of the original UD estimate of \mathbb{V}_e with a correction based on an upwind-biased estimate $(\mathbb{V}_P - \mathbb{V}_W)/\delta x$ of the gradient of \mathbb{V} multiplied by the distance $\delta x/2$ between node P and the east face [18]. In the TVD scheme, try to rearrange all the UD, LUD and QUICK schemes as follow,

$$\mathbb{V}_e = \mathbb{V}_P + \frac{\psi}{2} (\mathbb{V}_E - \mathbb{V}_P) \quad (20)$$

It is obviously understood that the UD scheme can obtain by replacing the value of ψ as zero. Nevertheless, by looking at the other schemes, it is seen that LUD scheme can be rewritten as

$$\mathbb{V}_e = \mathbb{V}_P + \frac{1}{2} \left(\frac{\mathbb{V}_P - \mathbb{V}_W}{\mathbb{V}_E - \mathbb{V}_P} \right) (\mathbb{V}_E - \mathbb{V}_P) \quad (21)$$

Which ψ is equal to $\mathbb{V}_P - \mathbb{V}_W / \mathbb{V}_E - \mathbb{V}_P$. For QUICK approximation expression, Equation (20) can be expressed as

$$\mathbb{V}_e = \mathbb{V}_P + \frac{1}{2} \left(\left(3 + \frac{\mathbb{V}_P - \mathbb{V}_W}{\mathbb{V}_E - \mathbb{V}_P} \right) \frac{1}{4} \right) (\mathbb{V}_E - \mathbb{V}_P) \quad (22)$$

Which, ψ is equal to $\left(3 + \frac{\mathbb{V}_P - \mathbb{V}_W}{\mathbb{V}_E - \mathbb{V}_P} \right) \frac{1}{4}$.

Based on the Equations 20-21, the value of function ψ can be estimated by the ratio of upwind-side gradient to downwind-side gradient. Therefore, in Equation 20, it can be expressed as $\psi = \psi(r)$, Where,

$$r = \frac{\mathbb{V}_P - \mathbb{V}_W}{\mathbb{V}_E - \mathbb{V}_P} \quad (23)$$

The general form of the east face value \mathbb{V}_e is given as below

$$\mathbb{V}_e = \mathbb{V}_P + \frac{\psi(r)}{2} (\mathbb{V}_E - \mathbb{V}_P) \quad (24)$$

In unstructured grid system the 24th equation is rewritten as follows

$$\nabla_i = \nabla_U + \frac{\psi(r)}{2} (\nabla_D - \nabla_U) \quad (25)$$

Where $\nabla_i, \nabla_U, \nabla_D$ are the values in face of the cell, upstream node point, and downstream node point, respectively. Because the value of upstream nodal is not available, so in the TVD scheme on an unstructured grid system, the value of r cannot be calculated in the same way as a structured grid system. Thus, an upstream ‘dummy’ node must calculate to solve the problem. The construction procedure of a dummy node can be found in Whitaker *et al.* [19] and Cabello *et al.* [20]. The illustration of dummy node is given in the Figure (3). By considering the average values of near nodal values, the value of r can written as,

$$r = \frac{\nabla_P - \nabla_B}{\nabla_A - \nabla_P} \quad (26)$$

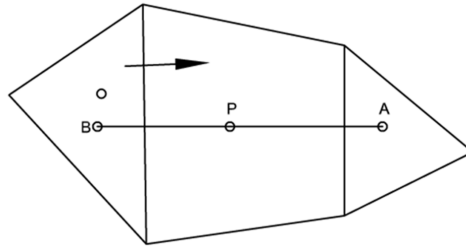


Fig. 3 Illustration of dummy node

Darwish and Moukalled [21] recommended the following method to estimate the value of r as,

$$r = \left[\frac{(2\nabla_P r_{PA})}{\nabla_A - \nabla_P} - 1 \right] \quad (27)$$

Which, r_{PA} is the vector of destination between nodes P and A . The flow can flux from p point to A point or contrariwise. It is important to note that in an unstructured grid system in order to give a general notation, it is better to use U and D instead of W and E nodes, respectively.

$$r = \left[\frac{(2\nabla_U r_{UD})}{\nabla_D - \nabla_U} - 1 \right] \quad (28)$$

The illustration of the node point in the unstructured grid system by considering the direction of flow is given in the Figure (4). More detail about r in the unstructured grid system can be found in the Darwish and Moukalled (2003).

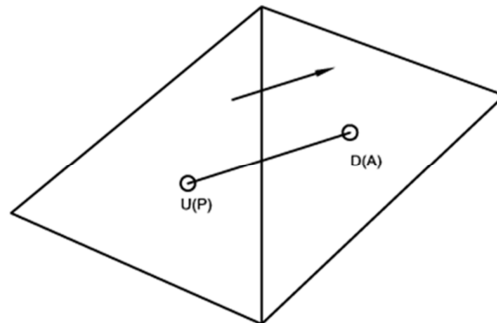


Fig. 4 Illustration of node point in unstructured grid system

5. Solution of Governing Equations

The final form of the governing equations is presented in this section. All of the equations are solved in explicit conditions. In order to develop the codes, MATLAB software is used. The final form of continuity equation is,

$$(h)^{t+1} = (h)^t - \frac{\Delta t}{A} \sum_{m=1}^M (L^m)_i [(ucos\theta + vsin\theta)_U h_U + \psi(r)((ucos\theta + vsin\theta)_D h_D - (ucos\theta + vsin\theta)_U h_U) / 2 + \Delta t S] \quad (29)$$

The last configuration of the momentum equation in the flow direction (x) is obtained as:

$$(u)^{t+1} = \{(hu)^t - \frac{\Delta t}{A} [\sum_{m=1}^M \frac{1}{2} g L^m (h^2_U cos\theta + \frac{\psi(r)((h^2_D cos\theta - h^2_U cos\theta))}{2}) + \sum_{m=1}^M L^m (hu^2 cos\theta)_U + \frac{\psi(r)((hu^2 cos\theta)_D - (hu^2 cos\theta)_U)}{2}] + \sum_{m=1}^M L^m (huvsin\theta)_U + \frac{\psi(r)((huvsin\theta)_D - (huvsin\theta)_U)}{2}]\} + \Delta t S / h^{t+1} \quad (30)$$

The final form of the momentum equation in the transect direction (y) is obtained as

$$(v)^{t+1} = \{(hv)^t - \frac{\Delta t}{A} [\frac{1}{2} g L^m ((h^2 sin\theta)_U + \frac{\psi(r)((h^2 sin\theta)_D - (h^2 sin\theta)_U)}{2}) + \sum_{m=1}^M L^m ((hv^2 sin\theta)_U + \frac{\psi(r)((hv^2 sin\theta)_D - (hv^2 sin\theta)_U)}{2})] + \sum_{m=1}^M L^m (huv cos\theta)_U + \frac{\psi(r)((huv cos\theta)_D - (huv cos\theta)_U)}{2}]\} + \Delta t S / h^{t+1} \quad (31)$$

As noted before, in order to examine the reliability and accuracy of results of the suggested model, Flow3D software was employed. The aforementioned software uses the NSE's system to solve CFD problems. In this paper, two hypothetical cases were solved by both of the Flow3D's NSE's and SWM. Flow3D software employs the FDM (or FVM) by an upwind scheme to solve the governing equations. Although this software presents both of the explicit and implicit solutions, but, most of the time for obtaining more reliable results (as instance, when require to determine sediment transport phenomenon), the governing equations should be employed in implicit condition. In this paper, for achieving more reliable results, the SWM and the NSE's in the above mentioned software were solved in explicit and implicit conditions, respectively. Meshing procedure is one of the vital steps for getting acceptable results in the CFD problems. In this step, the flow domain must be divided into tiny cells. However, it should be noted that in Flow3D software some limitations like the memory problem of computer, waste of the time, and wrong results could be happened by employing a very tiny cell size. The Flow3D software divides the domain of flow into the rectangular grid cells. In this study, a mesh generator component was developed to produce required meshes. Because the unstructured triangular grid cells have a better overlap in irregular and curvilinear geometries, so these kind of cells were employed for meshing procedure.

6. Numerical Investigation

Totally, two hypothetical cases were developed to investigate the numerical outcomes of the suggested model. The details of hypothetical cases and results are given in below.

6.1. Hypothetical Case 1

In this hypothetical case, a channel with 4 m length and 1 m width was assumed. The slope of the channel selected as 0.005 and 0.002 in the flow (x) and transect (y) directions, respectively. The non-uniform and unsteady flow developed by inlet hydrograph, which is illustrated in the Figure (5). The velocity of fluid in the flow (x) and transect (y) directions, assumed as 0.435 m/s and 0 m/s, respectively. Furthermore, the amounts of the Manning's roughness coefficient selected as 0.0025 and 0.009 for the bottom and sidewalls of the channel, respectively. The depth of the flow for initial and boundary conditions assumed as 0.06 m and the velocity components for initial and boundary conditions in the flow (x) and transect (y) directions, assumed as 0.435 m/s and 0 m/s, respectively.

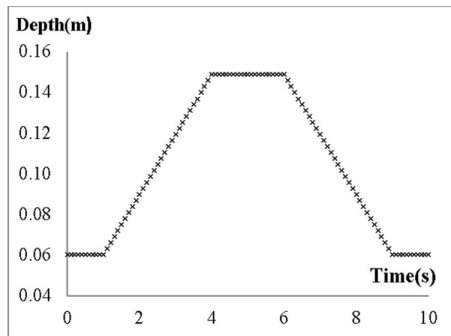


Fig. 5 Inlet hydrograph of hypothetical case 1

The numerical outcomes of suggested model by MATLAB, and simulation results with Flow3D software with the SWM (explicit) and NSE (implicit) are given in Figures 6-13. In Figures 6-7, the water surface profiles are presented at the two time steps (5 and 7), in the flow (x) direction, and in the middle point of the channel ($y=0.5$). Furthermore, the figures of water surface profiles in the transect (y) direction of the channel, and in the middle point of the channel ($x=2m$) at the two time steps (5 and 7) are presented in the Figures 8-9. It is worthwhile to mention that, in Figures of both of hypothetical cases, "Flow3DImp." is the symbol of numerical solutions of Flow3D by (NSE), "TVDCD" refers to the numerical results of the developed model by MATLAB, and "Flow3DExp." is the numerical solutions of Flow3D by SWM.

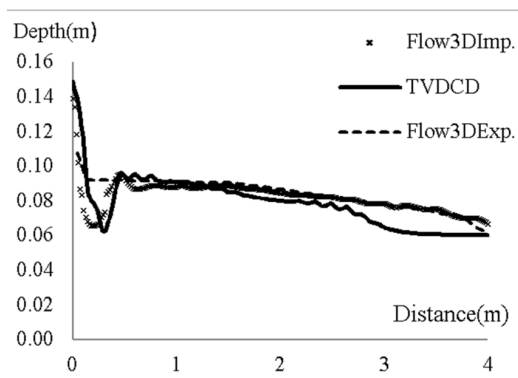


Fig. 6 Water surface profile in the flow direction at 5th sec

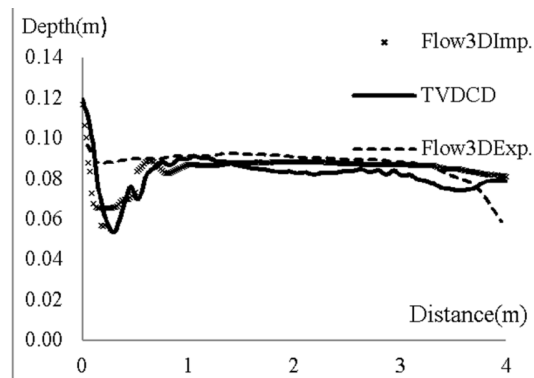


Fig. 7 Water surface profile in the flow direction at 7th sec

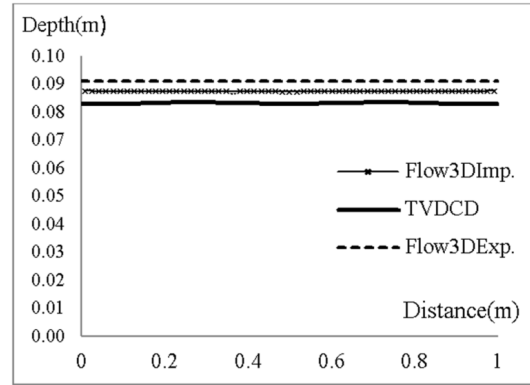
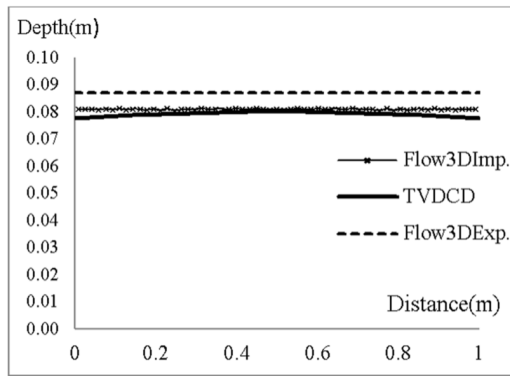


Fig. 8 Water surface profile in the transect direction at 5th sec **Fig. 9** Water surface profile in the transect direction at 7th sec
 According to the Figures 6-9, the suggested model by the authors can show better performance than the simulation results of Flow3D software in both of the flow (x) and transect (y) directions. With regards to the results, the developed model has better overlap by the Flow3D's implicit model instead of Flow3D's explicit model. In addition, one of the advantages of the suggested model is that this model (TVDCD) requires less size of meshes to obtain reliable results than Flow3D's explicit and implicit models. The dimensionless difference between numerical results of suggested model and explicit and implicit solutions of Flow3D software, were calculated as,
 Dimensionless Difference = (Flow3DImp. - TVDCD or Flow3DExp.) / Flow3DImp.

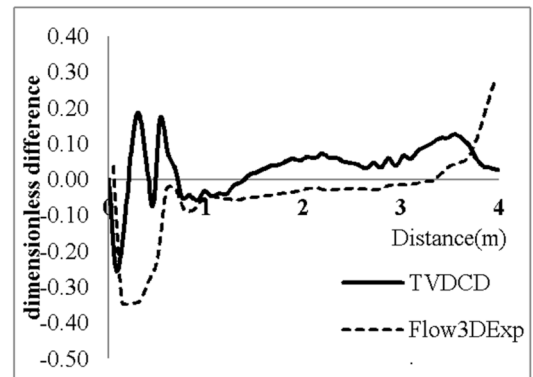
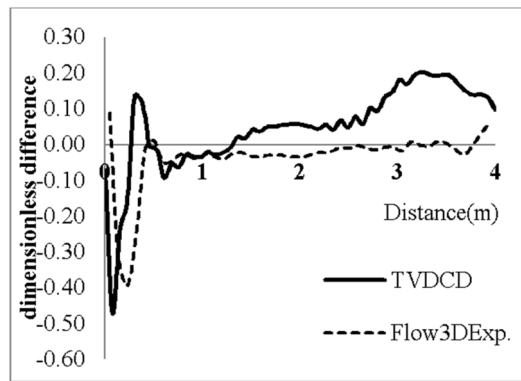


Fig. 10 Dimensionless difference of water surface profile in the flow direction at 5th sec **Fig. 11** Dimensionless difference of water surface profile in the flow direction at 7th sec

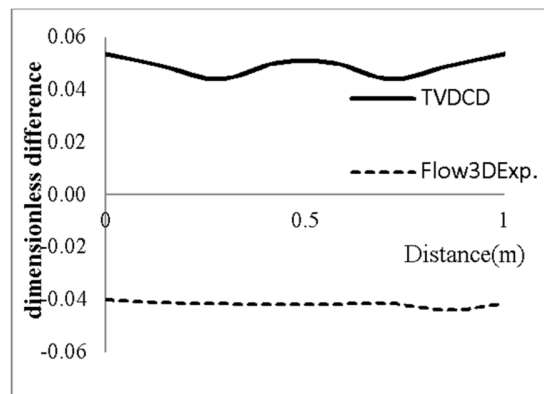
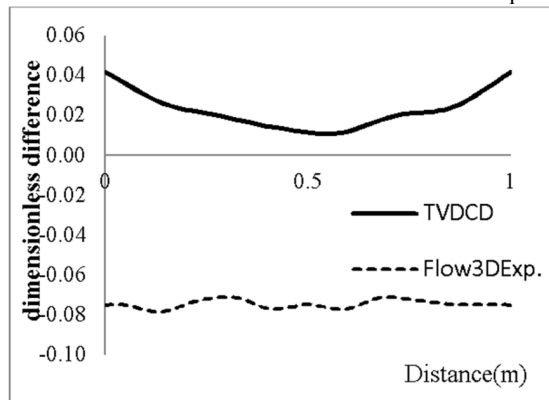


Fig. 12 Dimensionless difference of water surface profile in the transect direction at 5th sec **Fig. 13** Dimensionless difference of water surface profile in the transect direction at 7th sec

The dimensionless difference of water surface profiles in the flow (x) direction at the two time steps (5 and 7), are presented, in the Figures 10-11. Finally, the dimensionless difference of water surface profiles in the transect (y) direction in the middle point ($x=2$ m), for two various time steps (5 and 7), are given in the Figures 12-13. Like Figures 6-9, in dimensionless

figures it can be clearly understood that the developed model by MATLAB (TVDCD) shows better performance than Flow3D's explicit model (Flow3DExp). Because the Flow3D's SWM (explicit) cannot interpolate the values of inlet hydrographs in rough mesh size, so more tiny mesh cells must be selected. However, by using very tiny mesh cells, serious errors began to extend. Finally, by considering several trial and error methods in mesh sizes, the favorable mesh size selected for explicit solutions. Implicit model of Flow3D software cannot achieve reasonable results with the rough size of meshes. Furthermore, this software cannot solve the hypothetical case in two dimensions. If, the purpose of this research was prediction of water surface profiles in the flow (x) and depth of the flow (z) directions, Flow3D could develop 2D models. However, because in this work, preferred to consider the effect of the sidewalls too, therefore, developed models by Flow3D, was implemented in 3D. Hence, in the third direction, the number of meshes increased strongly.

6.2. Hypothetical Case 2

In the second hypothetical case, the length and width of the channel selected as 5 and 0.8 m, respectively. The Manning's roughness coefficient assumed as 0.003 and 0.009 for channel bed layer and sidewalls, respectively. The slope of the channel in the flow (x) and transect (y) directions selected as 0.005 and 0.002, respectively. The illustration of inlet hydrograph is given in the Figure(14). The values of velocity components in flow (x) and transect (y) directions, selected as 0.261 m/s and 0 m/s, respectively. For the initial conditions, the depth of the flow assumed as 0.028 and velocity components in flow (x) and transect (y) directions were selected as 0.261 m/s and 0 m/s, respectively. The illustration of inlet hydrograph is given in the Figure (14). In addition, like the previous hypothetical case , the illustrations of comparison between Flow3DImp., TVDCD and Flow3DExp. are yielded in the Figures 15-22. The illustrations of water surface profiles at the two time steps (4 and 6) in the flow direction and in middle point of the channel can be found in the Figures 15-16. Also, the illustration of water surface profiles in the transect (y) in the middle point at the two time steps (4 and 6) are given in the Figures 17-18. Finally, the dimensionless differences figures are presented in the Figures 19-22.

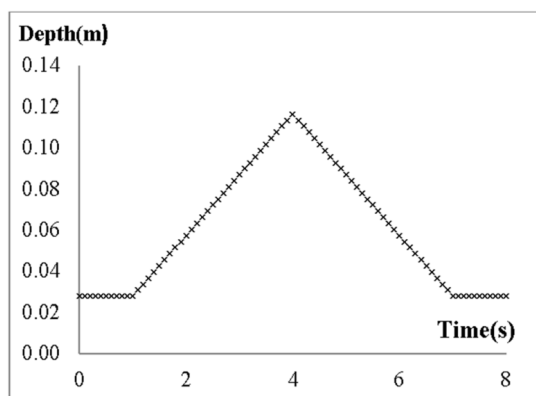


Fig. 14 Inlet hydrograph of hypothetical case 2

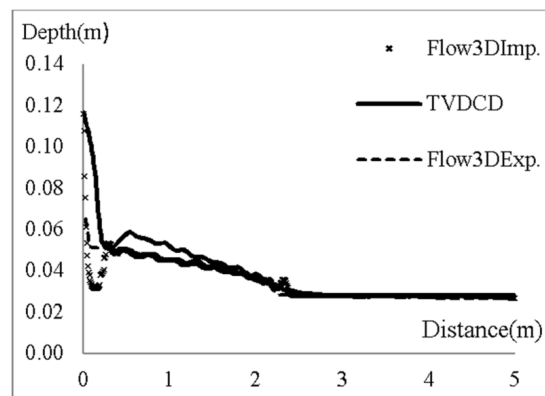


Fig. 15 Water surface profile in the flow direction at 4th sec

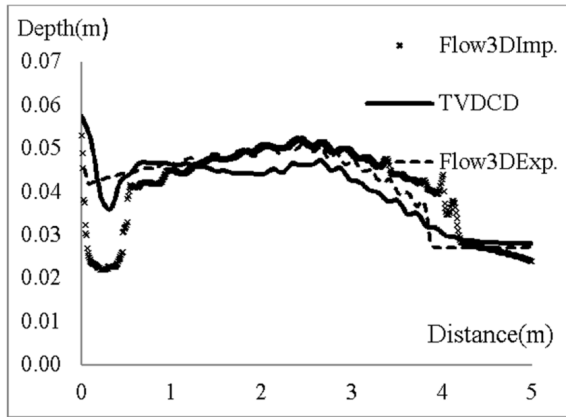


Fig. 16 Water surface profile in the flow direction at 6th sec

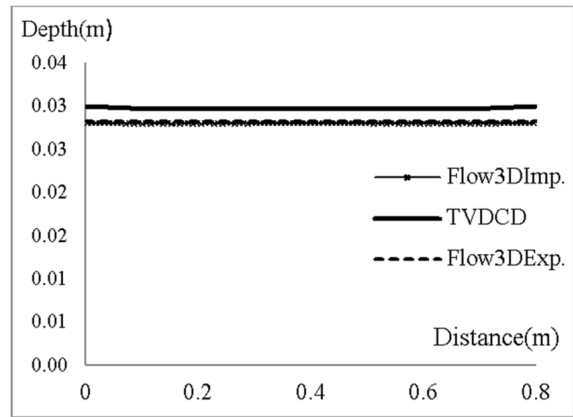


Fig. 17 Water surface profile in the transect direction at 4th sec

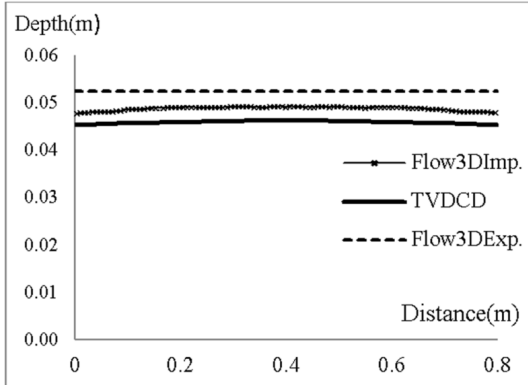


Fig. 18 Water surface profile in the transect direction at 6th sec

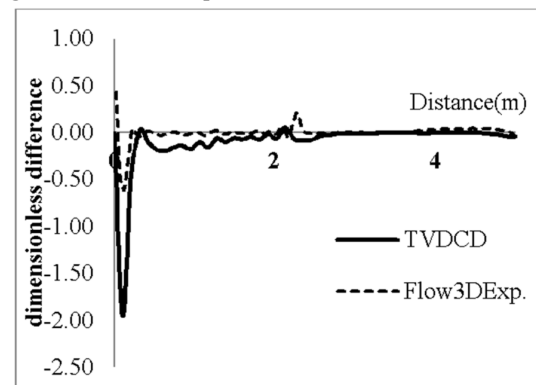


Fig. 19 Dimensionless difference of water surface profile in the flow direction at 4th sec

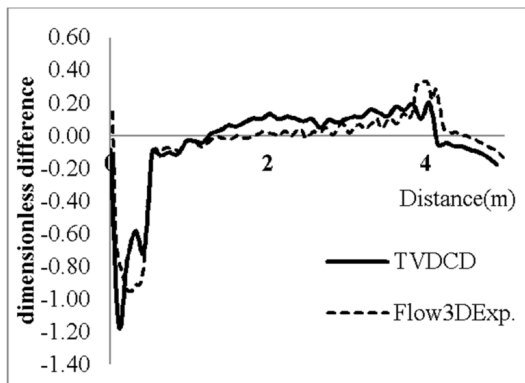


Fig. 20 Dimensionless difference of water surface profile in the flow direction at 6th sec

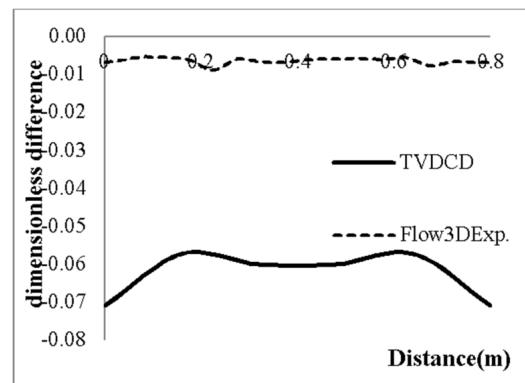


Fig. 21 Dimensionless difference of water surface profile in the transect direction at 4th sec

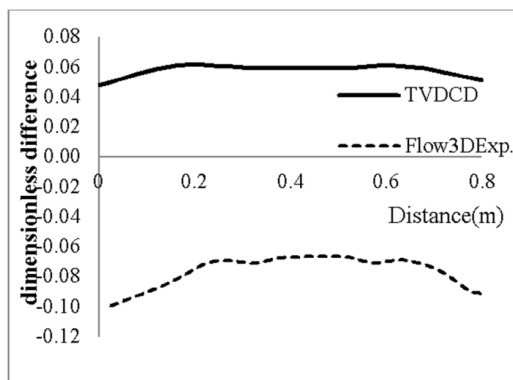


Fig. 22 Dimensionless difference of water surface profile in the transect direction at 6th sec

Based on the Figures 15-22, the suggested model by the authors, can calculate water surface profiles, correctly. The results of TVDCD in the flow (x) and transect (y) directions, and the results of Flow3DImp, are compatible with each other. For calculating a correct interpolation in the inlet hydrograph of the Flow3D models in the explicit and implicit conditions, strongly required to make a fine size of mesh. By using the very fine mesh numbers, sometimes computer cannot initiate to the simulation process. Finally, the developed model, could obtain better results that show good agreement by Flow3D's explicit and implicit models. It is important to mention that both of the hypothetical cases, were done on a computer with 2.4 GHz CPU and 4GB RAM. Moreover, Flow3D version 10.1 was employed to simulate the models.

7. Conclusions

The main purpose of this study is to present a 2D model to predict the water surface profiles in alluvial channels and rivers. The SWE's system was employed as a governing equation. The governing equations were discretized with a FVM in the explicit conditions. The class of TVD schemes was specially formulated to achieve oscillation-free solutions, which was proved to be useful in CFD simulations [18]. In spite of other researchers whom employed the total variation diminishing scheme by Riemann solvers, in this paper this scheme applied directly to the governing equations. In order to obtain a better compatibility with the physics of the problems, an unstructured triangular mesh generator was developed. One of the advantages of the suggested model is the size of applied meshes. The suggested model can obtain acceptable results with less number of meshes than Flow3D software. Moreover, developed model by the authors, which was solved in explicit conditions, ensure more coherence with Flow3D's implicit model instead of Flow3D's explicit model. It is worth pointing out that the developed model shows better performance than Flow3D's explicit model. As a suggestion for the future works, it would be worthwhile to develop a model of the TVD scheme in implicit conditions. Furthermore, it would be useful to investigate the suggested model by experimental data in open channels and rivers.

References

- [1] Wu, W., Vieira, D.A. and Wang, S.S.Y., One-dimensional numerical model for non-uniform sediment transport under unsteady flows in channel networks. *Journal of Hydraulic Engineering*, ASCE, 130(9), 914–923, 2004.
- [2] Seo, I.W, Jun, I. and Choi H.S., One-dimensional finite element model for suspended sediment transport analysis. *World City Water Forum*, 3107-3112, 2009.
- [3] Gharehbaghi, A. and Kaya, B., Simulation of bed changes in rivers with finite volume method by kinematic wave model. *International Journal of Engineering & Applied Sciences*, 3(3), 33-46, 2011.
- [4] Kaya, B. and Gharehbaghi, A., Modelling of sediment transport with finite volume method under unsteady conditions. *Journal of the Faculty of Engineering and Architecture of Gazi University*, 27 (4), 827-836, 2012.
- [5] Gharehbaghi, A., *Experimental and numerical study of sediment transport phenomenon*, LAMBERT Academic Publisher, 2016.

- [6] Kaya, B. and Gharehbaghi, A., Implicit solutions of advection diffusion equation by various numerical methods. *Australian Journal of Basic and Applied Sciences*, 8, 381-391, 2014.
- [7] Bradford, S.F. and Sanders, B.F., Finite-volume model for shallow-water flooding of arbitrary topography. *Journal of hydraulic engineering*, 128 (3), 2002.
- [8] Pan, C.H., Dai, S.Q. and Chen, S.M., Numerical simulation for 2d shallow water equations by using Godunov-Type scheme with unstructured mesh. *Journal of Hydrodynamics*, 18(4), 475-480, 2006.
- [9] Chen, S.C. and Peng, S.H., Two-dimensional numerical model of two-layer shallow water equations for confluence simulation. *Advances in Water Resources*, 29, 1608–1617, 2006.
- [10] Kesserwani, G. and Liang, Q.A., A discontinuous Galerkin algorithm for the two-dimensional shallow water equations. *Comput. Methods Appl. Mech. Engrg.*, 199, 3356–3368, 2010.
- [11] Touma, R. and Khankan, S., Well-balanced un staggered central schemes for one and two-dimensional shallow water equation systems. *Applied Mathematics and Computation*, 218, 5948–5960, 2012.
- [12] Canestrelli, A. and Toro, E.F., Restoration of the contact surface in FORCE-type centered schemes II: Non-conservative one- and two-layer two-dimensional shallow water equations. *Advances in Water Resources*, 47, 76–87, 2012.
- [13] Ata, R., Pavan, S., Khelladi, S. and Toro, E.F., A weighted average flux (WAF) scheme applied to shallow water equations for real-life applications. *Advances in Water Resources*, 6, 155–172, 2013.
- [14] Vasquez, J. A. and Walsh, B.W., CFD simulation of local scour in complex piers under tidal flow, 33rd IAHR Congress: Water Engineering for a Sustainable Environment, 2009.
- [15] Acharya, A. Experimental study and numerical simulation of flow and sediment transport around a series of spur dikes, PhD thesis, the University of Arizona, USA, 2011.
- [16] Afshar, H. and Hoseini, S.H., Experimental and 3-D Numerical Simulation of Flow over a Rectangular Broad- Crested Weir. *International Journal of Engineering and Advanced Technology*, 2(6), 2249 – 8958, 2013.
- [17] Cataño-Lopera, Y.A., Landry, B.J., Abad, J.D. and García, M.H., Experimental and numerical study of the flow structure around two partially buried objects on a deformed bed. *Journal of Hydraulic Engineering*, 269-283, 2013.
- [18] Versteeg, H.K, and Malalasekera W. An introduction to computational fluid dynamics the finite volume method , New York: Longman scientific & technical, 2th Ed., 2007.
- [19] Whitaker, D.L., Grossman, B. and LÖHNER, R., Two-dimensional Euler computation on a triangular mesh using upwind finite-volume scheme, AIAA, 27th Aerospace Science Meeting, Reno, NV., 1989.
- [20] Cabello, J., Morgan, K., and Lohner, R.A., Comparison of higher-order schemes in a finite volume solver for unstructured grids, AIAA, 25th Fluid Dynamics Conference, Colorado Springs, CO. 1994, 94-2295, 1994.
- [21] Darwish, M.S. and Moukalled, F., TVD schemes for unstructured grids., *Int. J. Heat Mass Transfer*, 46, 599–611, 2003.